Simultaneous improvement of the electrical conductivity and mechanical properties via double-bond introduction in the electrically conductive adhesives

Yu Su[1,2] · Lei Zhang[1,2] · Bing Liao[1,2] · Yu L. Mai[1,2] · Yong Q. Dai[1,2] · Wei Hu[1,2]

Abstract

For electrically conductive adhesives (ECAs), high electrical conductivity generally conflicts with excellent mechanical properties because electrical conductivity increases while desirable mechanical properties decrease with the increase in loading of conductive fillers or removal of lubricants on the silver filler surface. In this work, a method was developed to improve both the electrical conductivity and mechanical properties of the ECAs by introducing double bonds. Itaconic acid (IA) was used to replace the lubricant on the silver flake (Ag-F) surface, and acrylic acid (AA) was used as part of the ECA resin matrix. IA can replace the lubricant on the Ag-F surface, similar to other short-chain dibasic acids, to improve the ECA electrical conductivity. Furthermore, IA can be polymerized with AA to form covalent bonds between the silver flakes and the resin matrix, enhancing the mechanical properties of ECA. Compared with ECA filled with commercial silver flakes, the electrical conductivity of ECA filled with IA-treated silver flakes increased by ~21%, and the lap shear strength increased by ~29%.

1 Introduction

Electrically conductive adhesives (ECAs) are one of the most promising materials to replace tin/lead solder due to its advantages of lead-free content, rapid and simple development process, low process temperature, and high resolution for fine-pitch interconnect [1–3]. ECA is an environmentally friendly interconnect material, widely used in the connection and packaging of integrated circuits, liquid crystal displays, light-emitting diodes, solar cells, and other electronic devices and modules [4–7]. Although the ECAs offer many advantages, they have not completely replaced the traditional solders using ECAs. The major obstacles are that the electrical resistivity of ECAs is considerably higher than that of the solders, and the impact strength of ECAs is poorer, which limits the application of ECAs in advanced electrical

packaging [8–10]. Therefore, it is necessary to improve the electrical conductivity and mechanical properties of ECAs.

ECAs comprise a resin matrix, which provides mechanical strength and conductive fillers that offer electrical conduction [11, 12]. The effective electrical conductivity of ECA can be improved by adding conductive filler into the resin matrix, however, further increase in the amount of conductive filler does not lead to significantly increase the conductivity because the conductive network stabilizes after reaching the percolation threshold. Moreover, addition of the conductive filler deteriorates the mechanical properties and increases the viscosity, which negatively impacts the workability [13–15]. For silver-based ECAs, low conductivity is associated with the status of the silver filler surface. In order to prevent the aggregation of the silver filler and facilitate their dispersion into the resin matrix, majority of the commercially available silver fillers are covered with a long-chain fatty acid, which acts as a lubricant [16]. Unfortunately, this lubricant layer is nonconductive; therefore, it acts as an energy obstacle for electron tunneling among the neighboring silver fillers and can considerably increase the overall resistivity of the ECA [17]. Consequently, many methods have been reported to improve the electrical conductivity of the ECA by removing the lubricants such as in situ replacement of the lubricant by short-chain difunctional acids (such as succinic acid and adipic acid) [18–20],
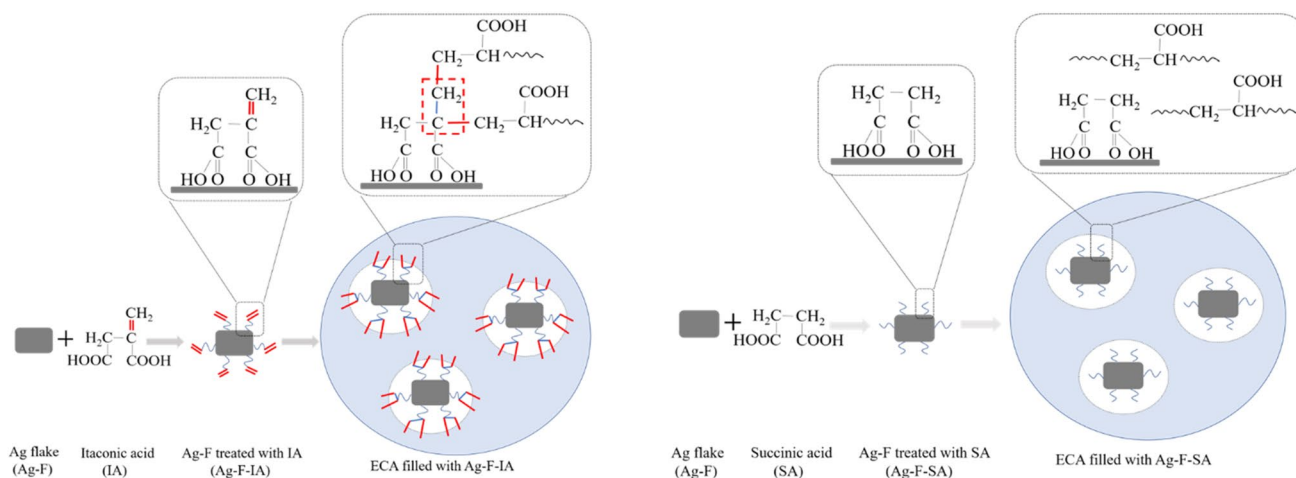
✉ Wei Hu
gracehz@126.com

1 Guangdong Research Institute of Petrochemical and Fine Chemical Engineering, Guangzhou 510665, China

2 Guangdong Province Key Laboratory of Industrial Surfactant, Guangdong Research Institute of Petrochemical and Fine Chemical Engineering, Guangzhou 510665, China

thermal decomposition of the lubricant [21–23] and iodination activation of the silver filler surface [24, 25]. However, the presence of long-chain fatty acids on the silver filler surface can enhance the compatibility between the silver fillers and the resin matrix, and improve the mechanical strength by increasing the interaction between the silver filler and the resin matrix through the intermolecular force. As the lubricant is removed from the surface of the silver fillers, the ECA viscosity increases and the lap shear strength may decrease significantly [18, 21, 25, 26]. ECAs provide not only electrical connections but also mechanical support. The excellent mechanical properties and bonding reliability of the ECAs provide the foundation for obtaining stable conductive performance and operational reliability in case of electronic products [27]. Adhesion strength is a crucial parameter of the ECAs; however, as mentioned above, there is an obvious contradiction between the conductivity and the adhesion strength. Therefore, the simultaneous improvement of the electrical conductivity and mechanical properties is a key challenge for ECAs.

In this work, short-chain difunctional acid containing an unsaturated double bond was used to in situ replace the lubricant on the silver flake surface, and acrylic acid (AA) was used as part of the resin matrix. The electrical conductivity of the ECA can be enhanced by removing the lubricant from the surface of the silver flake. Furthermore, the interaction between silver flakes and resin matrix can be improved by the covalent bond that polymerized of the AA and the unsaturated short-chain difunctional acid to enhance the mechanical properties of the ECA. The possible mechanism of this method is presented in Scheme 1.

2 Experimental

2.1 Materials

A commercial bisphenol A type epoxy resin (CYD 128, SINOPEC Baling Company, part of the resin matrix), triethanolamine (98%, Aladdin Biochemical Technology Co., Ltd., curing regent of epoxy resin), acrylic acid (AA; AR, Tianjin Damao Chemical Reagents Factory, another part of the resin matrix), azo-dis-isobutyronitrile (AIBN, 99%, Aladdin Biochemical Technology Co., Ltd., free radical polymerization initiator), acetone (AR, Guangzhou Chemical Reagent Factory, epoxy resin thinner and AIBN solvent), itaconic acid (IA; CP 99%, Aladdin Biochemical Technology Co., Ltd.), succinic acid (SA; AR, Tianjin Damao Chemical Reagents Factory), and anhydrous ethanol (AR, Guangzhou Chemical Reagent Factory) were used as received without any further treatment. Silver flake were purchased from Guangzhou Hongwu Materials Technology Co., Ltd.

2.2 Methods

2.2.1 Surface modification of silver flake

The silver flake was surface-modified with a 0.5 M solution of IA (or SA) in ethanol. The molar ratio of silver flake to acid was 1:1. The solution was sonicated for 90 min, and then allowed to stand for 20 h. The modified silver flake was subsequently purified twice by centrifuging at 2000 rpm for 5 min in the presence of ethanol, followed by drying in a vacuum oven at 30 °C for 12 h.

Scheme 1 Schematic of ECAs property improvement via double-bond introduction

2.2.2 Preparation of ECAs

ECA formulations were prepared by mixing precise quantities of silver flake with the resin matrix, which composed epoxy matrix (epoxy, triethanolamine, and acetone) and AA matrix (AA and AIBN). The mass ratio of epoxy matrix to AA matrix was 1:3. The epoxy resin, AA, and acetone were blended for 1 min in a vacuum rev-rot gravity mixer (VM300SA2, Mianyang Sinomix Science and Technology Co., Ltd). Next, the silver flake was added to the viscous paste and mixed for 5.5 min. Finally, triethanolamine and AIBN were added followed by mixing for another 1 min. The mass ratio of epoxy resin, triethanolamine, and acetone was 100:15:2, whereas that of AA to AIBN was 50:1. The silver flake loading of the ECA was 80% by weight.

All curing processes are performed in a box oven under air at 200 °C for 30 min.

2.2.3 Characterization

The morphologies of silver flakes and composites were studied by field emission scanning electron microscopy (SEM, HITACHI SU-8010). Energy dispersive X-ray spectroscopy (EDS) was used to analyze the quantitative element contents of C, O, and Ag on the silver flake surface (HITACHI SU-8010). Further, the acceleration voltage was 20 kV, and the results were estimated based on the measurements conducted at 3 measurement spots. The size distribution of silver flakes was studied using the laser diffraction particle size analyzer (Malvern Mastersizer3000). Differential scanning calorimetry (DSC, TA Q2000) was used to detect and characterize the lubricants on the silver flakes and cured ECAs. For this purpose, the temperature was increased from 50 to 400 °C at a heating rate of 10 °C/min. Raman spectra were obtained by the Raman spectrometer (HORIBA LabRam HR Evolution). The 633-nm line of the He–Ne laser was used for the experiments. X-ray photoelectron spectroscopy (XPS) measurements were carried out on a K-Alpha + X-ray photoelectron spectrometer (Thermo Fisher Scientific) with a Mono Al Kα X-ray source (1486.6 eV photons). The thermal decomposition behavior of the lubricant on the silver flakes was characterized by thermogravimetric analysis (TGA Q50) under nitrogen. Further, the temperature was increased from 30 to 700 °C at a rate of 10 °C/min. The ECA resistivity was measured by a four-point probe meter (Nanjing Daming Instrument Co., Ltd. DMR-1C), and the resistivity ρ was calculated as follows:

$$\rho = R \times d, \tag{1}$$

where R and d denote the sheet resistance and thickness of the sample, respectively. The thickness of the cured samples was measured by a micrometer gauge, and the average sheet resistance and thickness of each sample were estimated based on the measurements conducted at five points on the sample surface. Three parallel samples were prepared for each ECA. The ECA samples for the lap shear strength test were prepared according to the National Standard of the People's Republic of China GB7124-2008 (EQV ISO 4587:2003). In accordance with this standard, the adhesive was used to bond two stainless steel panels with the following dimension: thickness of 1.6 ± 0.1-mm, width of 25 ± 0.25-mm, and length of 100 ± 0.25-mm. The bonding part on the sample was $B = 12.5 \pm 0.25$ mm in width and $L = 25 \pm 0.25$ mm in length. The prepared sample was cured at 200 °C for 30 min. The panels were pulled apart with an electronic universal testing machine (MTS, CMT4204) at a pull rate of 5 mm/min. Five parallel samples were prepared for each ECA, and the lap shear strength (τ) was calculated as follows:

$$\tau = F/(B \times L), \tag{2}$$

where F is the force applied to break apart the bonded panels, B is the width of the bonded area, and L is the length of the bonded area.

3 Results and discussion

Three types of silver flakes were prepared (Table 1): silver flake without any treatment, denoted as Ag-F; Ag flake treated with saturated SA, denoted as Ag-F–SA; and Ag flakes treated with unsaturated IA, denoted as Ag-F–IA.

3.1 Morphology and particle size distribution of silver flakes

The morphology and particle size of the silver filler considerably influence the electrical conductivity and mechanical properties of the ECA. The silver flakes were treated by sonication and centrifugation. We used SEM and the laser diffraction particle size analyzer to investigate the three aforementioned silver flakes to observe the changes in morphology and particle size. The results are presented in Fig. 1. The SEM images denote that the treated and untreated silver flakes exhibit similar morphologies, exhibiting an irregular shape with a diameter of approximately 2 μm. There was no significant difference in the particle size distribution curves of the three silver flakes. This result suggests that the treatment has little effect on the morphology and the size distribution of the silver flakes.

Table 1 Three types of silver flakes

Silver flakes	Sample code	Acid	
		Acid name	Chemical structure
Commercial silver flake without any treatment	Ag-F	×	×
Silver flake treated with SA	Ag-F–SA	Succinic acid	(structure shown)
Silver flake treated with IA	Ag-F–IA	Itaconic acid	(structure shown)

Fig. 1 SEM images of **a** Ag-F, **b** Ag-F–SA, and **c** Ag-F–IA. **d** size distribution of Ag-F, Ag-F–SA and Ag-F–IA
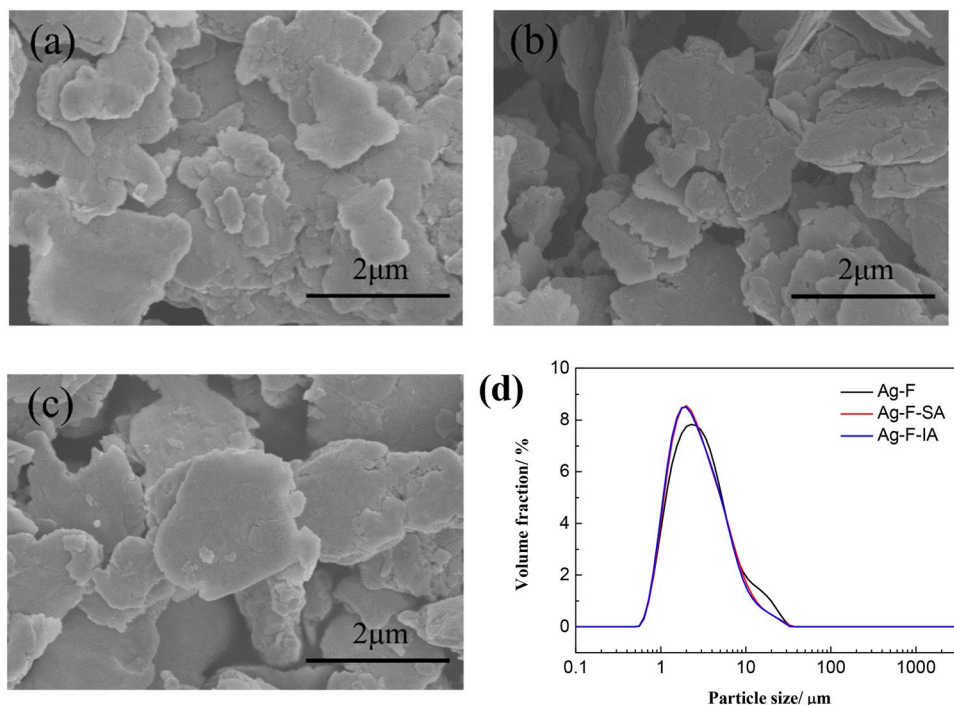
3.2 Characterization of organics on the surface of silver flakes

DSC is a convenient and reliable technique to characterize the lubricants on the silver flakes. Ag-F, Ag-F–SA, and Ag-F–IA were respectively studied by DSC in two different atmospheres: nitrogen (N_2) and oxygen (O_2). The results are shown in Fig. 2 and Table 2. An exothermic peak is observed for the sample under the oxygen atmosphere; however, it is absent for the sample under the nitrogen atmosphere. Furthermore, Ag-F, Ag-F–SA, and Ag-F–IA show exothermic peaks at different temperatures. This result indicates that the exothermic peaks are related to the oxidation process of the different organic materials on the surfaces of different silver flakes.

To characterize the chemical structures of the organic materials on the surfaces of silver flakes, Raman spectroscopy was applied to investigate these three silver flakes. Figure 3a shows the spectra of Ag-F–SA, Ag-F, and SA. The bands at 2931, 1634, 1403, and 953 cm^{-1} in the Ag-F–SA spectrum can be attributed to C–H stretching, C=O stretching, C–H flexural, and C–COO$^-$ stretching vibrations, respectively. The band at 335 cm^{-1} can be attributed to the pseudocycle deformation vibration. This bond was reported by Moskovits and Suh to demonstrate that both carboxylate groups of succinic acid are bound to the silver surface [28]. Figure 3b shows the spectra of Ag-F–IA, Ag-F, and IA. The bands at 2931, 1591, and 1540 cm^{-1} in the Ag flakes-IA spectrum can be attributed to C–H stretching, C=O stretching, and C=C stretching vibrations, respectively. Methylene twisting and wagging can be observed at 1295

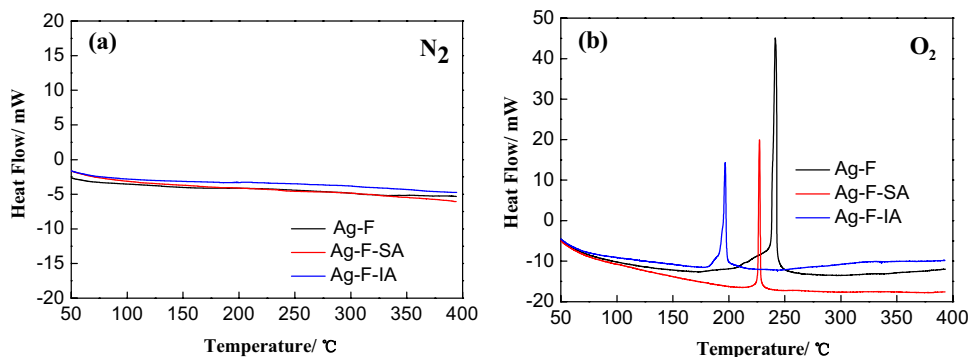**Fig. 2** DSC curves of Ag-F, Ag-F–SA, and Ag-F–IA in **a** N_2 and **b** O_2

Table 2 DSC exothermic peaks and reaction heat of Ag flakes

	Peak temperature (°C)	Reaction heat (J/g)
Ag-F	241.5	119.2
Ag-F–SA	227.4	36.0
Ag-F–IA	196.7	53.1

matter on the surface of the silver flake decreased after being treated with SA or IA. Ag-F–SA demonstrated the lowest total mass of organic matter. Furthermore, the mass of organic matter on the surface of Ag-F–IA was higher than that on the surface of Ag-F–SA.

EDS was used to detect the quantitative element content of the silver flakes before and after treatment (the detailed data are presented in Table 3) [29]. Ag-F contained 2.30

and 1362 cm⁻¹, respectively [23]. The band at 636 cm⁻¹ can be attributed to the C=O deformation vibration of C=C–COOH. Thus, Raman results confirm that the SA and IA are adsorbed on the silver flake surface after treatment.

3.3 Organic content on the surface of the silver flakes

Organic matter is insulated, and the conductivity of the ECA is affected by the organic content on the surface of the silver flakes. TGA was used to detect the amount of organic matter on silver flakes. Figure 4 shows the weight loss of three silver flakes during heating. Ag-F denoted a weight loss of ~1% at temperatures of 150 to 300 °C; Ag-F–IA denoted a weight loss of ~0.7% at temperatures of 130 to 400 °C; and Ag-F–SA denoted a weight loss of ~0.5% at temperatures of 130 °C to 400 °C. These results demonstrate the presence of a lubricant layer on the Ag-F surface. The mass of organic
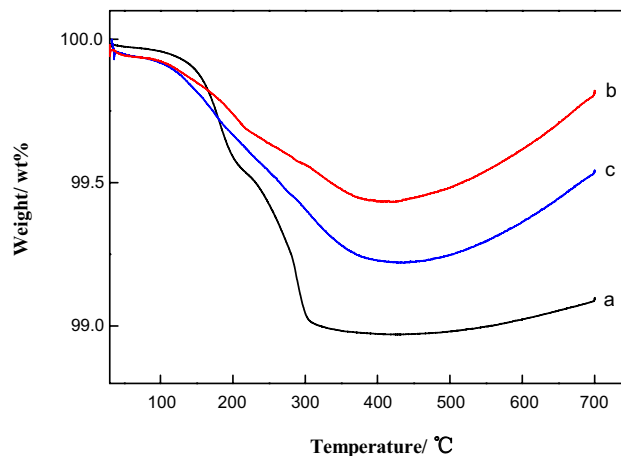

Fig. 4 TGA curves of (a) Ag-F, (b) Ag-F–SA, and (c) Ag-F–IA

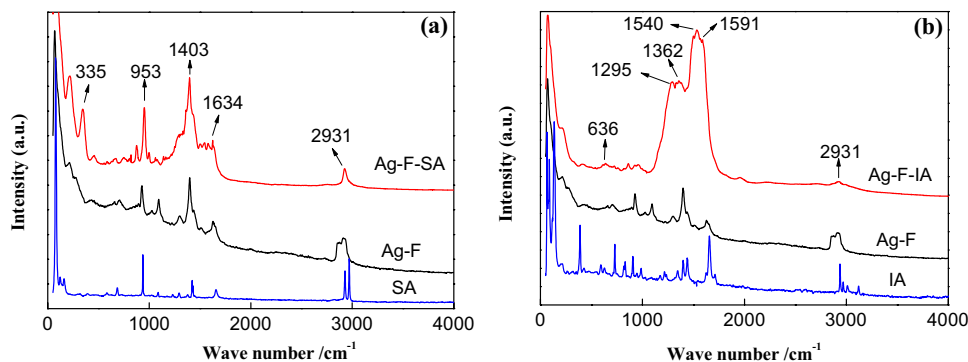**Fig. 3** Raman spectra for **a** Ag-F–SA, Ag-F, and SA; **b** Ag-F–IA, Ag-F, and IA

Table 3 Detailed quantitative element content of silver flakes

	C/wt%	O/wt%	Ag/wt%
Ag-F	2.30 (±0.13)	0.31 (±0.01)	97.39 (±0.14)
Ag-F–SA	1.40 (±0.01)	0.22 (±0.03)	98.38 (±0.04)
Ag-F–IA	2.06 (±0.43)	0.31 (±0.01)	97.62 (±0.44)

wt% of C, 0.31 wt% of O, and 97.39 wt% of Ag; Ag-F–SA contained 1.40 wt% of C, 0.22 wt% of O, and 98.38 wt% of Ag; and Ag-F–IA contained 2.06 wt% of C, 0.31 wt% of O, and 97.62 wt% of Ag. After treatment with IA, the carbon content of the silver flake decreased to 2.06 wt%. In case of SA, the decrease in carbon content was even more obvious. This result shows that the organic matter content on the surface of the silver flakes decreased after treatment. The residue amount of organic material on Ag-F–SA was minimal. These results agree with the TG test results.

The results demonstrate that the surface status of the silver flakes can be effectively changed via treatment. The

organic content on the surface of the silver flakes is different after the treatment.

3.4 Interaction between short-chain difunctional acids and silver flakes

To characterize the interaction between short-chain difunctional acids and silver flakes, the surface chemical structures of Ag-F, Ag-F–SA, and Ag-F–IA were analyzed by XPS. Figure 5 shows the XPS spectra of the silver flakes. In case of Ag-F after treatment with short-chain difunctional acids, the C1s core-level spectra and O1s core-level spectra changed, indicating that the chemical environment on the surface of the silver flake was changed. The C1s core-level spectra of Ag-F–SA can be curve-fitted into three peak components at binding energies of ~284.8, 286.3, and 288.1 eV, which can be attributed to the C–C, C–O, and C=O species, respectively (Fig. 5f). The C1s core-level spectra of Ag-F–IA can be curve-fitted into four peak components at binding energies of ~284.7, 285.0, 286.4, and 288.0 eV,
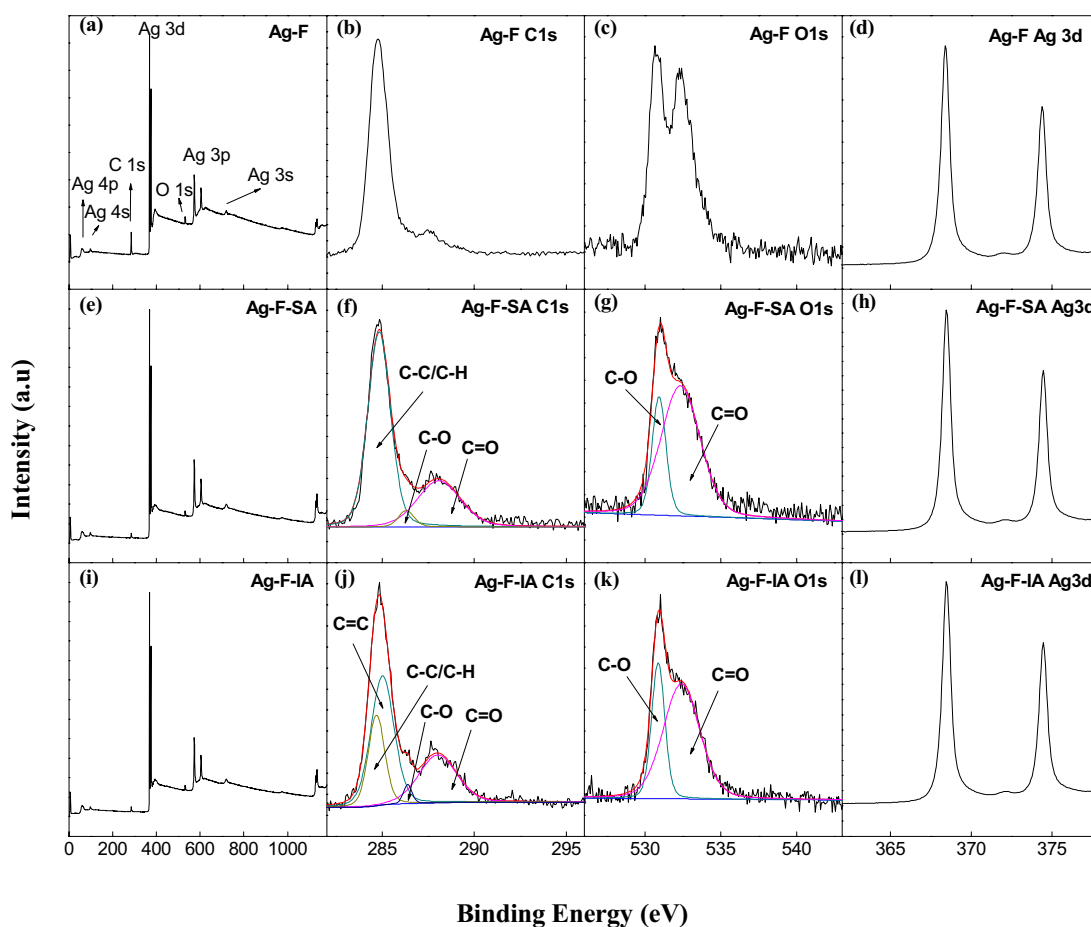

Fig. 5 XPS spectra: **a–d** are wide-scan spectra, C1s core-level spectra, O1s core-level spectra, and Ag 3d spectra of Ag-F, respectively; **e–h** are wide-scan spectra, C1s core-level spectra, O1s core-level spectra, and Ag 3d spectra of Ag-F–SA, respectively; and **i–l** are wide-scan spectra, C1s core-level spectra, O1s core-level spectra, and Ag 3d spectra of Ag-F–IA, respectively

which can be attributed to the C–C, C=C, C–O, and C=O species, respectively (Fig. 5j). Generally, the C1s peak of the free carboxylic acid exhibits a binding energy that is greater than but close to 289 eV [30]. In Fig. 5f, j, no signal greater than but close to 289 eV is obviously present, indicating that there is no free carboxylic acid on the surface of Ag-F–SA or Ag-F–IA. Thus, the two carboxyl groups of SA and IA are coordinated to the silver flake surface. When the metal surface adsorbs the organic difunctional acid, there are two different coordination types between the carboxylate and the metal [31, 32]: (1) monodentate coordination, in which the C=O still exists, the two oxygen atoms of COO– are not equivalent, and there are two O 1 s peaks at binding energies of ~531 and 533 eV; (2) bidentate coordination, also known as chelation coordination, in which the two oxygen atoms of COO– are equivalent and there is a single O $1s$ peak at approximately 531 eV in the XPS spectra. The O $1s$ spectra of Ag-F–SA can be curve-fitted into two peak components at binding energies of ~530.9 and 532.3 eV, which can be attributed to the C–O and C=O species, respectively (Fig. 5g). The O1s spectra of Ag-F–IA can be curve-fitted into two peak components at binding energies of ~530.9 and 532.4 eV, which can be attributed to the C–O and C=O species, respectively (Fig. 5k). Thus, SA and IA interact with the silver flake similarly, indicating that they are adsorbed on the silver flakes in monodentate coordination.

3.5 DSC analysis of the cured ECAs

The cured ECAs were studied using DSC under nitrogen atmosphere, and the results are presented in Fig. 6. An exothermic process can be observed after 220℃ (Figs. 6b, 6d, and 6f). This exothermic process is exhibited by all ECAs that can be attributed to the decomposition of the resin matrix and the oxidation of silver. The ECAs containing Ag-F and Ag-F–SA undergo glass transition at 135–190 ℃ (Figs. 6a and 6c). However, the ECA containing Ag-F–IA did not exhibit the glass transition in this temperature range (Fig. 6e). Glass transition is a macroscopic manifestation of the movement of the polymer molecular segments. The glass transition temperature is the lowest temperature at which the molecular chain segment can move and its height is directly related to the molecular chain. In ECA containing Ag-F–IA, AA copolymerized with the IA adsorbed on the surface of silver flakes. Further, the movement of molecular segments was restricted owing to the coordination between IA and silver flakes. Therefore, the glass transition of the ECA containing Ag-F–IA should be achieved at a high temperature. The resin matrix began to decompose at 220° C, hence, the glass transition process cannot be observed in the DSC curve of ECA filled with Ag-F–IA. This also indicates that the IA on the silver surface polymerizes with AA to achieve a covalent connection.

3.6 Bulk electrical resistivity and lap shear strength of the ECAs

Figure 7 depicts the bulk electrical resistivity and lap shear strength of the as-made ECAs. The electrical resistivity of the ECA filled with untreated silver flake is ~1.00×10^{-4} Ω·cm. After the silver flake was treated with short-chain difunctional acids, the electrical resistivity of the ECAs significantly decreased. The ECA filled with Ag-F–SA denoted an electrical resistivity of ~8.5×10^{-5} Ω·cm. Furthermore, the ECA filled with Ag-F–IA showed an lower electrical resistivity of ~7.9×10^{-5} Ω·cm. Compared to the ECA filled with Ag-F, the electrical conductivity of ECA filled with Ag flakes–IA increased to ~21%. The electrical property of ECA was expected to improve with the decreasing thickness of the lubricant layer because the lubricant on the silver flake surface was nonconductive [20, 33, 34]. After the Ag-F was treated with SA or IA, the amount of organic matter on the surface of the silver flake decreased. Therefore, the electrical resistivity of the ECA filled with Ag-F–SA was lower than that of ECA filled with Ag-F, a similar phenomenon could be observed in case of ECA filled with Ag-F–IA. The electrical resistivity of ECA filled with Ag-F–IA was lower than for ECA filled with Ag-F–SA even though the amount of organic matter on Ag-F–IA was greater than on Ag-F–SA. This behavior may be attributed to the introduction of double bonds on the silver flake surface. This mechanism would increase the interaction between the silver flake and resin matrix, giving the ECA better effective electrical conductivity. As shown in Fig. 7, the ECA filled with Ag-F–IA showed the highest lap shear strength (8.97 MPa), followed by the ECA filled with Ag-F (6.94 MPa) and ECA filled with Ag-F–SA (4.73 MPa). The lap shear strength of the ECA filled with Ag-F–IA was enhanced by ~29% when compared with the ECA filled with Ag-F. This result can be attributed to the fact that ECAs are composite materials. Their mechanical strength is strongly correlated with the interaction between the conductive filler and resin matrix. In particular, the mechanical strength increases with the increasing strength of bonding (in this case chemical bonding) between the filler and the matrix [35]. When ECA filled with Ag-F–IA was cured, the IA adsorbed on the silver flake and polymerized with the AA that constituted the resin matrix, forming chemical bonds between the conductive fillers and resin matrix. In contrast, the interaction between the silver fillers and the resin matrix in the ECA filled with Ag-F was the intermolecular interaction of the long-chain fatty acids with the resin matrix. In the ECA filled with Ag-F–SA, this intermolecular force was even weaker. Therefore, the ECA filled with Ag-F–IA showed the highest lap shear strength. Furthermore, the ECA filled with Ag-F–IA provide improved electrical conductivity and mechanical support.
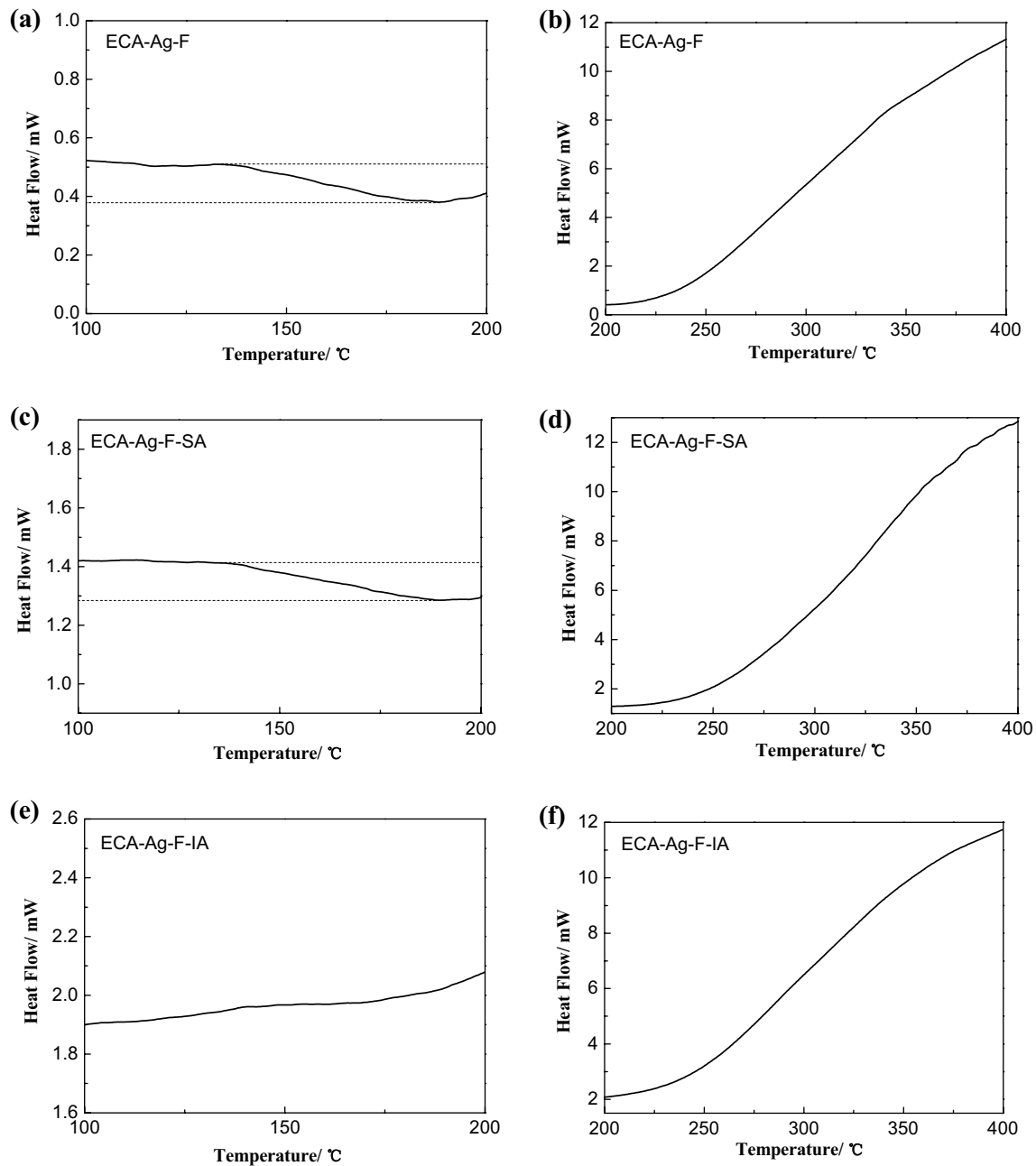
Fig. 6 DSC curves: **a**, **b** cured ECA filled with Ag-F; **c**, **d** cured ECA filled with Ag-F–SA; **e**, **f** cured ECA filled with and Ag-F–IA

4 Conclusion

The introduction of double bonds simultaneously improved the electrical conductivity and mechanical properties of the ECAs. Ag-F (long-chain fatty acids on the surface), Ag-F–SA (SA on the surface), and Ag-F–IA (IA on the surface) were prepared and used as the conductive fillers of ECAs. AA was used as part of the ECA resin matrix, and the ECA filled with Ag-F–SA showed better electrical conductivity but poorer mechanical properties than ECA filled with

Ag-F. However, the electrical conductivity of ECA filled with Ag-F–IA was 21% better than that of the ECA filled with Ag-F, and its lap shear strength was ~29% stronger than that of ECA filled with Ag-F. Similar to other short-chain difunctional acids, IA can replace the lubricant on the silver flake surface to improve the electrical conductivity of the ECAs. Furthermore, IA can be polymerized with AA in the resin matrix to form covalent bonds between the silver flake and the resin matrix, enhancing the mechanical properties of the ECAs.
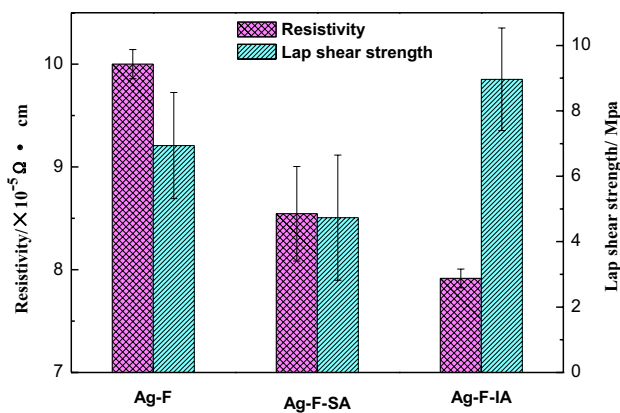
Fig. 7 Bulk electrical resistivity and lap shear strength of ECAs filled with Ag-F, Ag-F–SA, and Ag-F–IA

References

1. Y. Li, K.-S. Moon, C.P. Wong, Electronics without lead. Science **308**, 1419 (2005)
2. M.J. Yim, Y. Li, K.-S. Moon, K.W. Paik, C.P. Wong, Review of recent advances in electrically conductive adhesive materials and technologies in electronic packaging. J. Adhesion. Sci. Technol. **22**, 1593 (2008)
3. R. Zhang, J. C. Agar, C.P Wong, Recent Advances on Electrically Conductive Adhesives. in *Proceedings of the 2010 12th Electronics Packaging Technology Conference, EPTC*, 2010, pp. 696–704
4. I. Mir, D. Kumar, Recent advances in isotropic conductive adhesives for electronics packaging applications. Int. J. Adhes. Adhes. **28**(7), 362 (2008)
5. Y. Tao, Y. Chang, Y. Tao, H. Wu, Z. Yang, Self-healing ag/epoxy electrically conductive adhesive using encapsulated epoxy-amine healing chemistry. J. Appl. Polym. Sci. (2015). https://doi.org/10.1002/app.41483
6. T.H. Chiang, Y.C. Lin, Y.F. Chen, E.Y. Chen, Effect of anhydride curing agents, imidazoles, and silver particle sizes on the electrical resistivity and thermal conductivity in the silver adhesives of LED devices. J. Appl. Polym. Sci. (2016). https://doi.org/10.1002/app.43587
7. T. Geipel, M. Meinert, A. Kraft, U. Eitner, Optimization of electrically conductive adhesive bonds in photovoltaic modules. IEEE J. Photovolt. **8**(4), 1074 (2018)
8. Y. Guan, X. Chen, F. Li, H. Gao, Study on the curing process and shearing tests of die attachment by Ag–epoxy electrically conductive adhesive. Int. J. Adhes. Adhes. **30**, 80 (2010)
9. H.-W. Cui, D.-S. Li, Q. Fan, H.-X. Lai, Electrical and mechanical properties of electrically conductive adhesives from epoxy, micro-silver flakes, and nano-hexagonal boron nitride particles after humid and thermal aging. Int. J. Adhes. Adhes. **44**, 232 (2013)
10. R.R. Gomatam, E. Sancaktar, Dynamic fatigue and failure behavior of silver-filled electronically conductive adhesive joints at ambient environmental conditions. J. Adhesion. Sci. Technol. **18**(7), 731 (2004)
11. H.-M. Ren, Y. Guo, S.-Y. Huang, K. Zhang, M.M.F. Yuen, X.-Z. Fu, S. Yu, R. Sun, C.-P. Wong, One-step preparation of silver hexagonal microsheets as electrically conductive adhesive fillers for printed electronics. ACS Appl. Mater. Interfaces **7**(24), 13685 (2015)
12. Y.-H. Ji, Y. Liu, G.-W. Huang, X.-J. Shen, H.-M. Xiao, S.-Y. Fu, Ternary Ag/epoxy adhesive with excellent overall performance. ACS Appl. Mater. Interfaces **7**(15), 8041 (2015)
13. B.M. Amoli, A. Hu, N.Y. Zhou, B. Zhao, Recent progresses on hybrid micro–nano filler systems for electrically conductive adhesives (ECAs) applications. J. Mater. Sci. **26**(7), 4730 (2015)
14. D. Chen, X. Qiao, X. Qiu, F. Tan, J. Chen, R. Jiang, Effect of silver nanostructures on the resistivity of electrically conductive adhesives composed of silver flakes. J. Mater. Sci. **21**, 486 (2010)
15. Y.H. Wang, A. Huang, H. Xie, J.Z. Liu, Y.Z. Zhao, J.Z. Li, Isotropical conductive adhesives with very-long silver nanowires as conductive fillers. J. Mater. Sci. **28**, 10 (2017)
16. D. Lu, Q.K. Tong, C.P. Wong, A study of lubricants on silver flakes for microelectronics conductive adhesives. IEEE Trans. Compon. Pack. Technol. **22**(3), 365 (1999)
17. Y. Li, K.-S. Moon, A. Whitman, C.P. Wong, Enhancement of electrical properties of electrically conductive adhesives (ECAS) by using novel aldehydes. IEEE Trans. Compon. Pack. Technol. **29**(4), 758 (2006)
18. Y. Li, K.-S. Moon, C.P. Wong, Electrical property improvement of electrically conductive adhesives through in-situ replacement by short-chain difunctional acids. IEEE Trans. Compon. Pack. Technol. **29**(1), 173 (2006)
19. H.-W. Cui, Q. Fan, D.-S. Li, Surface functionalization of micro silver flakes and their application in electrically conductive adhesives for electronic package. Int. J. Adhes. Adhes. **48**, 177 (2014)
20. Y. Li, K.-S. Moon, H. Li, C.P. Wong, Conductivity improvement of isotropic conductive adhesives with short-chain dicarboxylic acids. in *Proceedings of the Electronic Components & Technology Conference. IEEE*, 2004, pp. 1959–1964.
21. C. Li, Q. Li, L. Cheng, T. Li, H. Lu, L. Tang, K. Zhang, J. Zhang, Z. Li, Y. Yao, Conductivity enhancement of polymer composites using high-temperature short-time treated silver fillers. Compos. A **100**, 64 (2017)
22. D. Lu, C.P. Wong, Thermal decomposition of silver flake lubricants. J. Therm. Anal. Calorim. **61**(1), 3 (2000)
23. R. Zhang, W. Lin, K.-S. Moon, C.P. Wong, Fast preparation of printable highly conductive polymer nanocomposites by thermal decomposition of silver carboxylate and sintering of silver nanoparticles. ACS Appl. Mater. Interfaces. **2**(9), 2637 (2010)
24. C. Yang, Y.-T. Xie, M.-F. Yuen, B. Xu, B. Gao, X. Xiong, C.P. Wong, Silver surface iodination for enhancing the conductivity of conductive composites. Adv. Funct. Mater. **20**(16), 2580 (2010)
25. C. Li, Q. Li, X. Long, T. Li, J. Zhao, K. Zhang, J. Zhang, Z. Li, Y. Yao, In-situ generation of photosensitive silver halide for improving the conductivity of electrically conductive adhesives. ACS Appl. Mater. Interfaces. **9**, 29047 (2017)
26. C. Wan, H. Wang, B. Du, W. Ling, Y. Fu, H. Liu, Effect of Ag morphology and surface treatment on electrically conductive adhesive. Electron. Process Technol. **32**(2), 72 (2011)
27. G. Xiao, E. Liu, T. Jin, X. Shu, Z. Wang, G. Yuan, X. Yang, Mechanical properties of cured isotropic conductive adhesive (ICA) under hygrothermal aging investigated by micro-indentation. Int. J. Solids. Struct. **122–123**, 81 (2017)
28. M. Moskovits, J.S. Suh, Conformation of mono- and dicarboxylic acids adsorbed on silver surfaces. J. Am. Chem. Soc. **107**, 6826 (1985)
29. H.-M. Ren, K. Zhang, Y.M. Matthew, X.-Z. Fu, R. Sun, C.P. Wong, Preparation and performance of Ag-coated Cu flakes filled epoxy as electrically conductive adhesives. J. Solid State Light. (2014). https://doi.org/10.1186/s40539-014-0010-9

30. X. Chen, Z. Zhang, F. Xiao, The interaction mechanism of dicarboxylic acids and electrically conductive adhesives. J. Funct. Mater. **42**(5), 947 (2011)

31. L.H. Dubois, B.R. Zegarski, R.G. Nuzzo, Spontaneous Organization of carboxylic acid monolayer films in ultrahigh vacuum. Kinetic constraints to assembly via gas-phase adsorption. Langmuir **2**, 412 (1986)

32. M. Wühn, J. Weckesser, Ch Wöll, Bonding and orientational ordering of long-chain carboxylic acids on Cu(111): investigations using X-ray absorption spectroscopy. Langmuir **17**, 7605 (2001)

33. C.P. Wong, D. Lu, Q.K. Tong, Lubricants of silver fillers for conductive adhesive applications. Adhesive Joining and Coating Technology in Electronics Manufacturing, 1998. in *Proceedings of 3rd International Conference on IEEE*, 1998.

34. D. Lu, C.P. Wong, Characterization of silver flake lubricants. J. Therm. Anal. Calor. **59**(3), 729 (2000)

35. F. Tan, X. Qiao, J. Chen, H. Wang, Effects of coupling agents on the properties of epoxy-based electrically conductive adhesives. Int. J. Adhes. Adhes. **26**(6), 406 (2006)